The Crab Nebula and its Mysteries: Some facts and puzzles

Martin C. Weisskopf, NASA/MSFC

Abstract

We discuss and summarize five results that we and various colleagues have produced over the last few years in the study of the wonderful, yet enigmatic, Crab Nebula and its pulsar. The results, in turn, have to do with the geometry inferred from *Chandra* X-ray observations, the surprising results of pulse phase polarimetry at 1.4 GHz, the search for an X-ray location of the gamma-ray flares for which we have *Agile* and *Fermi* to thank, and seeing if the optical and infrared inner knot might be the location of these flares.

Introduction

So much has been written about the Crab that another introduction seems superfluous. Rather, I would refer the reader to two outstanding references by Buhler and Blandford [2] and Hester [3].

Geometry

This work was performed with my colleagues R.F. Elsner, J.J. Kolodziejczak, S.L. O'Dell, and A. F. Tennant [5]. Figure 1 shows a *Chandra* image which used the low-energy transmission grating together with the High Resolution Camera keep the flux to a reasonable value. The asymmetry of the ellipse with respect to the pulsar motivated this exercise.

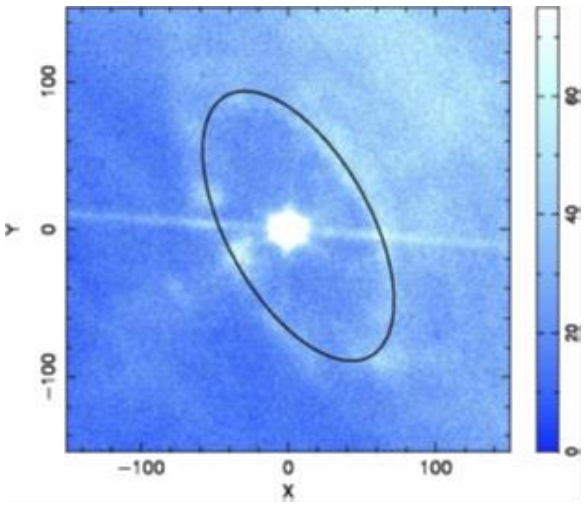

Figure 1. X-ray image of the inner region of the Crab Nebula and its pulsar taken with the *Chandra* LETG/HRC. The long trace extending to the NE (N is up and E is to the left) and SW of the pulsar is the zero-order image of the dispersed pulsar spectrum.

The elliptical shape suggests that the feature is a ring in the coordinate system defined by the spin axis of the pulsar. The displacement of the ellipse with respect to the pulsar implies that the plane of the ring is displaced from the plane perpendicular to the spin axis of the pulsar.

Using the peak surface brightness of the flux in the ring to establish the distance from the pulsar one obtains R=13.3″ (0.12 pc), θ=119.1°, ψ =298.4°, ξ = 1.04″ (0.01 pc), and λ = 4.5° where these various parameters are defined in Figure 2. ψ is the position angle of the projected spin axis and θ is the polar angle from the spin axis to the line of sight. Figure 3 shows the resulting geometry

when viewed in the plane defined by the spin axis and the pulsar. Since we find that the inner ring is located above the pulsar and along the spin axis it is natural to assume that π-λ is the angle of the magnetic field with respect to the spin axis as shown in Figure 3.

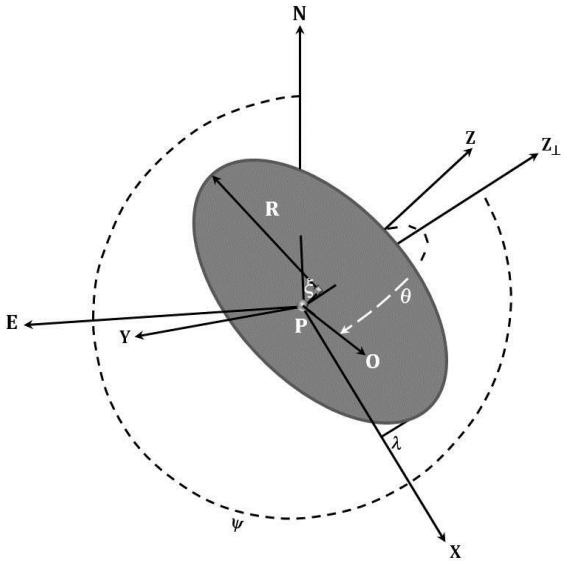

Figure 2. Simple geometrical model

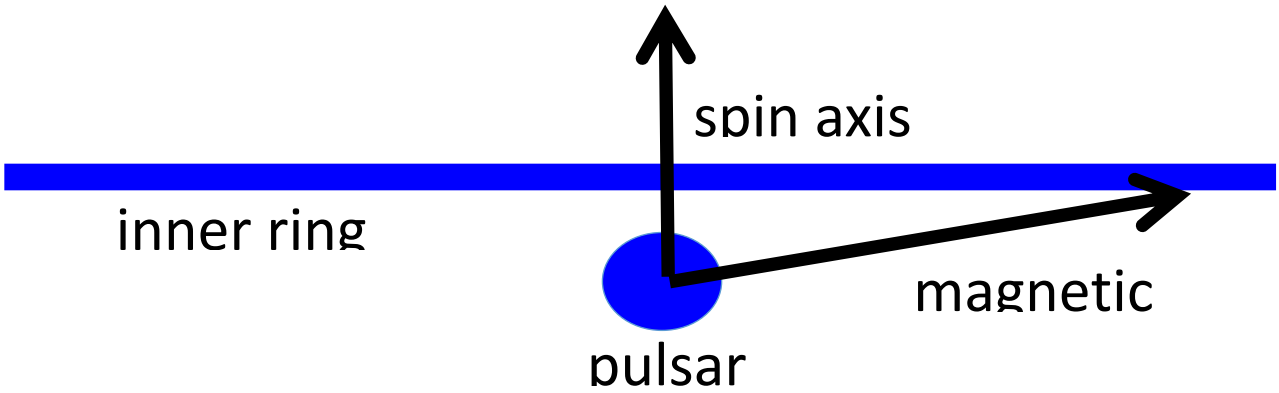

Figure 3. Inferred relative locations and orientations of the ring, the pulsar and its spin and magnetic axes.

Radio Polarization as a Function of Pulse Phase

This work was performed with my colleagues A. Slowikowska, B. Stappers, A. Harding, S. O'Dell, R. Elsner and A. van der Horst [4].

It may come as a surprise to find that high-time-resolution observations of the Crab pulsar in the radio band were not performed until near the end of the 20-th century (Moffett and Hankins in 1998.) and that and that the time resolution of 256 μsec only provided a small handful of samples within the very narrow primary and secondary pulses. We therefore decided to improve on these measurements by improving the resolution by a factor of 63 to 4μsec using the Westerbork Radio Telescope at 1.4 GHz. The results are shown in Figure 4.

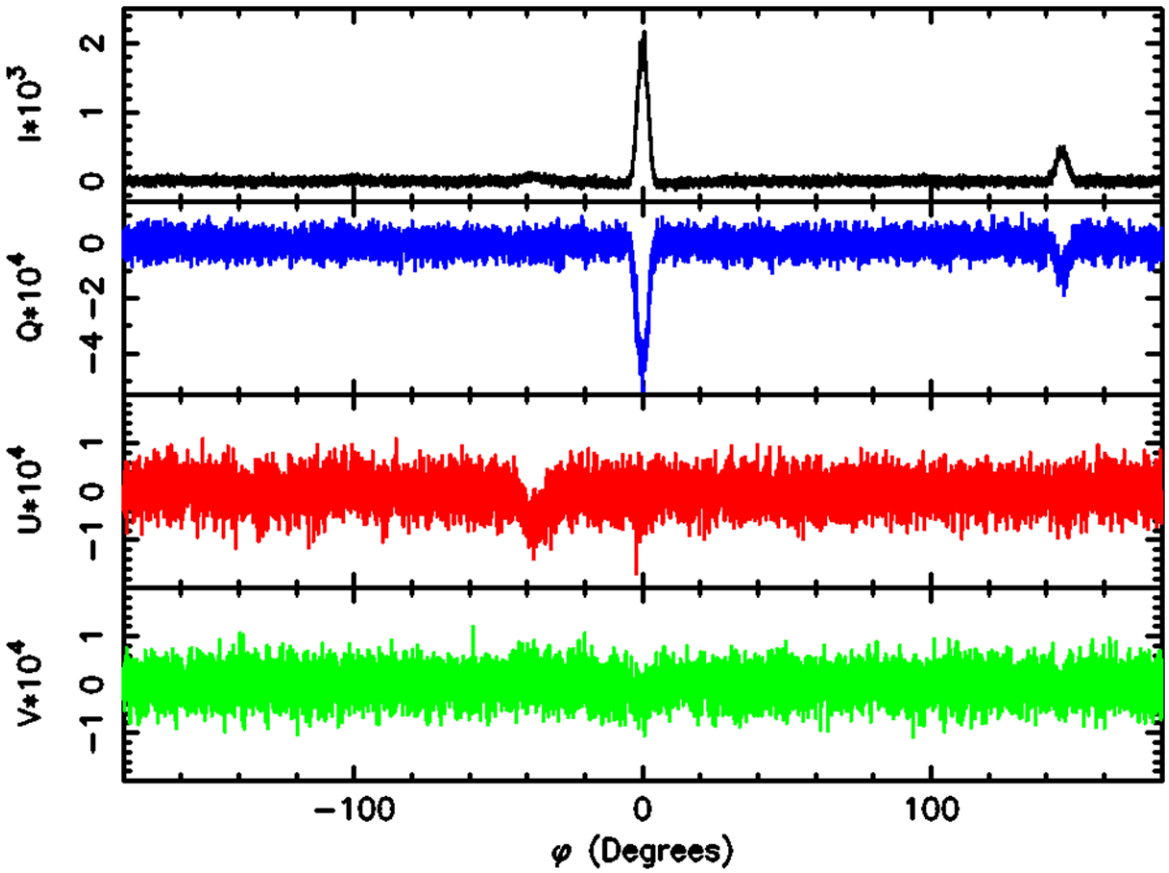

Figure 4. Stokes parameters I, Q, U, and V as a function of pulse phase at 1.4GHz.

Three principal features of the pulsation are visible in these data: the main pulse (MP) at 0°, the interpulse pulse (IP) at 145° and the low-frequency precursor (LFP) at about -18°. The MP and IP properties are very similar whereas LFP polarization properties are different from these. Moreover, there is no variation of the position angle through the various pulse components!

Now we know that the MP and IP appear at ~ same phase from radio to γ-ray and various models (slot gap, outer gap, and current sheet) all account for the γ-ray light curve. These models all produce the γ-rays at high altitudes which in turns suggests that the radio emission is also produced at high altitudes. But, if true, then one predicts distinct sweeps of the position angle and dips in linear polarization on the edge of the pulse peaks (as in the optical) which are not observed!

Search for the origin of the γ-ray flare of 2011 April

This work was performed with my colleagues A.F. Tennant, J. Arons, R. Blandford, R. Bühler, P. Caraveo, C.C. Cheung, E. Costa, A. De Luca, C. Ferrigno, H. Fu, S. Funk, M. Habermehl, D. Horns, J.D. Linford, A. Lobanov, C. Max, R. Mignani, S. L. O'Dell, R. Romani, E. Striani, M. Tavani, G.B. Taylor, Y. Uchiyama, and Y. Yuan [8].

.

Gamma-ray flares from the Crab Nebula were detected by both *Agile* and *Fermi*-LAT (Tavani et al., Abdo et al.). These and subsequent observations determined that the increase in flux was not in the pulsed emission, indicating a nebular origin. Moreover, the time scale of the flux variations indicated that the size of the emitting region is very small, about 2×10^{16} cm (0.3″) at 2 kpc. Finally, the spectra of the flares indicated a synchrotron origin and, as the time scale of the flares was longer than the synchrotron lifetime, one requires an acceleration mechanism to maintain the radiating particles. The question as to where within the nebula these flares are taking place is very relevant to further understanding.

We were very fortunate to obtain *Chandra* observations of the Crab during a flaring episode on 2011, April. Figure 5 shows the *Fermi*-LAT photon flux as a function of time with the time of the *Chandra* observations indicated.

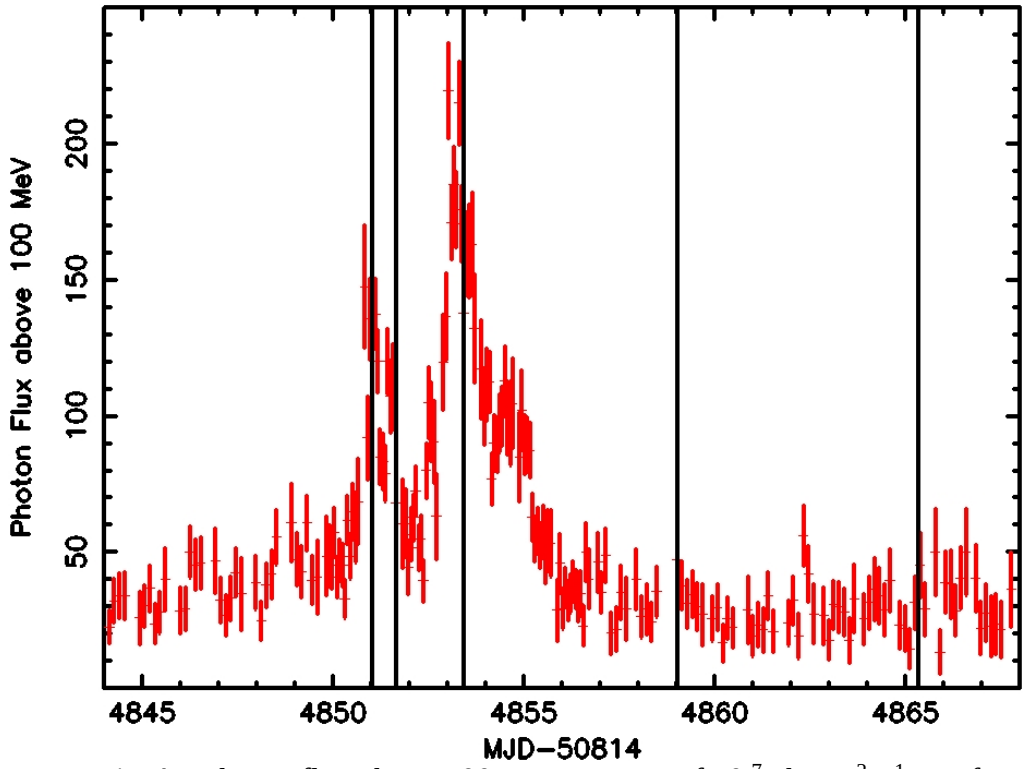

Figure 5. *Fermi*-LAT photon flux above 100 MeV in units of 10^{-7} ph cm^{-2} s^{-1} as a function of time. The solid vertical lines indicate when *Chandra*-ACIS observations were taken.

We analyzed the *Chandra* images for variability over the 5 observations. The pixels with the most significant variations are shown in the image in Figure 6. However, allowing for the number of pixels, none of these variations were significant at even the 99% confidence level. Specifically there was an 11% probability that we would find three or more events exhibiting the measured variability. It is interesting to note that all three most significant variations are associated with the inner ring. The data were also examined for variability within each of the 5 observations. Once again there was no compelling evidence for variability

.

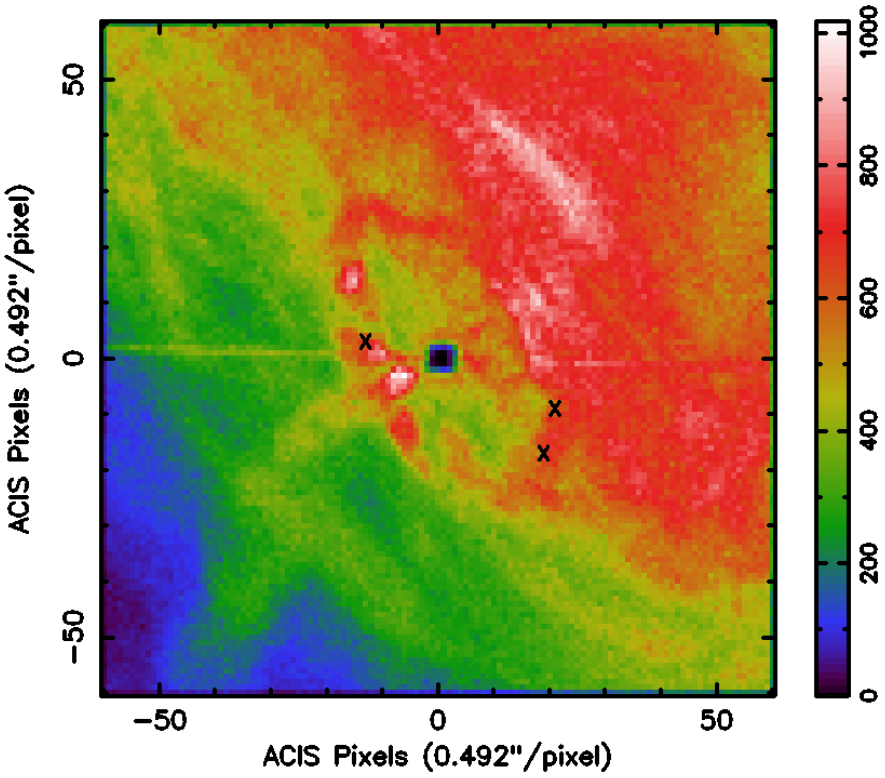

Figure 6. Summed image of the 5 *Chandra* observations. The color bar shows the summed counts per ACIS pixel. North is up and the pulsar is at the origin. The pulsar flux is so high that pileup removes the image. The nearly horizontal streak through the pulsar is the out-of-time image of the pulsar. The three X symbols indicate the location of the three most statistically significant variations observed.

What about the Inner Knot?

This work was performed with my colleagues A. Rudy, D. Horns, A. De Luca, J. Kolodziejczak, A. Tennant, Y. Yuan, R. Bühler, J. Arons, R. Blandford, P. Caraveo, E. Costa, S. Funk, A. Lobanov, C. Max, M. Mayer, R. Mignani, S. L. O'Dell, R. Romani, and M. Tavani [7].

An interesting feature of the Crab system is the inner knot, located *in projection* approximately 0.65″ southeast of the pulsar. The feature is very small and thus consistent with the apparent spatial size of the flare-emitting region inferred from time variability. Figure 7 shows Keck images which clearly resolve the feature. *Chandra* is not able to do so although we did set an upper limit to the X-ray flux. Using HST and Keck we performed detailed characterization of the properties of the knot. As part of this work we introduced a new approach for analyzing time series of astronomical images based on singular value decomposition techniques. We found that the knot's size and brightness are well correlated with the apparent separation from the pulsar. Unfortunately, we were not able to determine a strong correlation with the characteristics of the knot and γ-ray flares. Indeed as shown in Figure 8, there appears to be a total lack of correlation with the strongest γ-ray fluxes practically at the extremes of the measured separation.

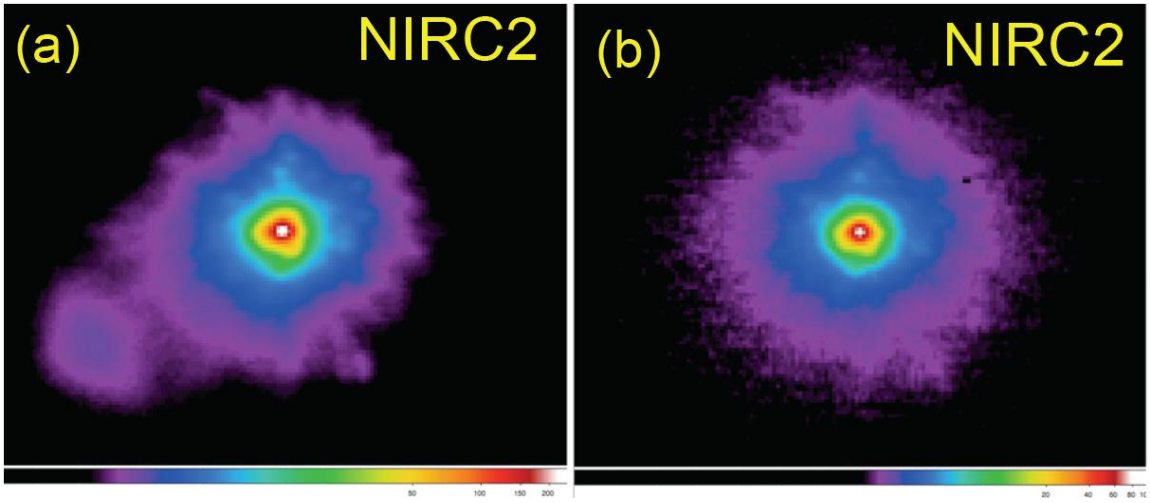

Figure 7. Keck observations with the Near Infrared Camera 2 (NIRC2) of the Crab pulsar (a, left) and a comparison start (b. right). The pixels are 0.01″ and the field of view is 10″×10″.

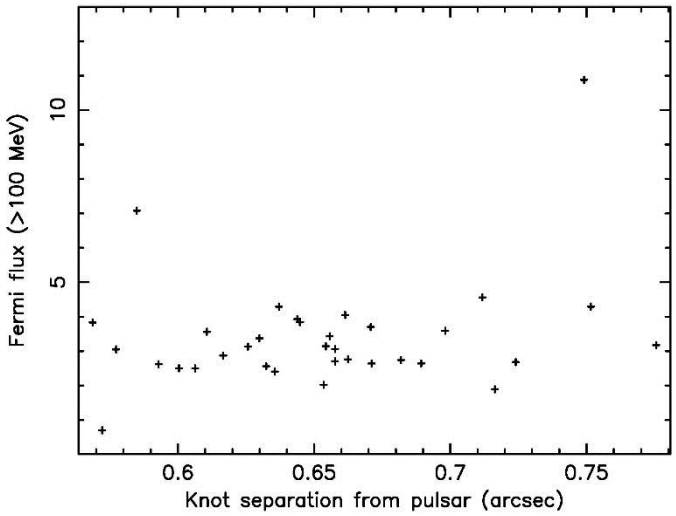

Figure 8. *Fermi*-LAT 12-hr average fluxes in units of 10^{-6} ph/cm^2/s centered on times of measurements of the pulsar-knot separation.

Summary and conclusions

Despite being one of the most studied objects the Crab Nebula and its pulsar are well from being understood. We hope that these vignettes of more recent observations of the system serve to emphasize this point. We feel that the next steps need to work on theory that attempts to tie all of these and other studies together in one beautiful astrophysical package. We hope that this overview serves to continue to stimulate such efforts.

Acknowledgements

We have identified in the text large number of collaborators that have contributed to these studies. We owe a deep debt of gratitude to all of them

References

1. Abdo, A., Ackermann, M., Aiello, M., et al., 2011, Science, 331,739
2. Bühler, R. & Blandford, R., 2014, Reports on Progress in Physics, 77, 066901
3. Hester, J., 2008, Annual Review of Astronomy & Astrophysics, 46, 127
4. Rudy, A., Horns, D., De Luca, A., et al., 2015, ApJ, 811, 24
5. Slowikowska, A., Stappers, B., Harding, A., et al., 2015, ApJ, 799, 70
6. Tavani, M., Bulgarelli, A., Vittorini, V. et al., 2011, Science, 331, 736
7. Weisskopf, M.C., Elsner, R.F., Kolodziejczak, J.J., et al., 2012, ApJ, 746, 41
8. Weisskopf, M.C., Tennant, A.F., Arons, J., et al., 2013, ApJ, 765, 56